Available online at www.sciencedirect.com

SciVerse ScienceDirect

Ceramics International 38 (2012) 1707–1711

CERAMICS INTERNATIONAL

www.elsevier.com/locate/ceramint

Short communication

Influence of V_2O_5 as an effective dopant on the sintering behavior and magnetic properties of $NiFe_2O_4$ ferrite ceramics

Jinjing Du *, Guangchun Yao, Yihan Liu, Jia Ma, Guoyin Zu

School of Materials and Metallurgy, Northeastern University, China

Received 8 July 2011; received in revised form 26 August 2011; accepted 30 August 2011
Available online 6 September 2011

Abstract

Samples with small amounts of V_2O_5 (0, 0.5, 1.0, 2.0, 2.5 wt%, respectively) were prepared via ball-milling and two-step sintering from commercial powders (i.e., Fe_2O_3, NiO and V_2O_5). Micro-structural features, phase transformation, sintering behavior and magnetic properties of V_2O_5-doped $NiFe_2O_4$ composite ceramics have been investigated by scanning electron microscopy (SEM), X-ray diffraction (XRD), thermal dilatometer and vibrating sample magnetometer (VSM), respectively. Morphology and the detecting result of thermal dilatometer show that V_2O_5 can promote sintering process, the temperature for 2.5 wt% V_2O_5-doped samples to reach the maximum shrinkage rate is 59 °C lower than that of un-doped samples. With an increase of V_2O_5 from 0 wt% to 2.5 wt%, the apparent activation energy decreased from 813.919 kJ/mol to 298.806 kJ/mol. The early-stage synthesis process of un-doped ceramic samples and 2.5 wt% V_2O_5-doped samples are mainly controlled by grain boundary diffusion and volume diffusion, respectively. Increasing V_2O_5 content, residual magnetization ratio (Mr/Ms) and coercivity (Hc) elevate, meanwhile, saturation magnetization decreases.

Keywords: A. Sintering; C. Magnetic properties; D. Spinels; Ceramics; Vanadium pentoxide (V_2O_5)

1. Introduction

The materials science literature is rich in papers dealing with structural, physical, chemical, electrical and magnetic properties of phases belonging to spinel structure type, with general chemical formulae $M^{2+}O{\cdot}M_2^{3+}O_3$ (where M^{2+} = Mg, Mn, Fe, Co, Cu, Zn, Ni and M^{3+} = In, Al, V, Cr, Mn, Fe) [1,2]. Nickel ferrite ($NiFe_2O_4$) is one of the most important spinel ferrites as well as a typical spin soft-magnetic ferrite. It has cubic inverse spinel structure showing ferromagnetism. The ferromagnetism originates from magnetic moment of anti-parallel spins between Fe^{3+} ions at tetrahedral sites and Ni^{2+}ions at octahedral sites [3,4]. The cubic inverse spinel structure provides a better chemical stability in the molten cryolite-alumina bath [5–7]. So nickel ferrite ($NiFe_2O_4$) can be used as a promising candidate for green inert anodes. It can produce environment-friendly O_2 gas during electrolysis instead of greenhouse gases. Nickel ferrite ($NiFe_2O_4$), as a semiconductor, has attracted considerable attention in the field of technological application with a wide range of frequencies extending from microwave to radio frequency. These characteristics are strongly dependent upon several factors such as chemical composition, method of preparation, stoichiometry, sintering time and temperature, sintering atmosphere, porosity and substitution of different ions [8].

Many efforts have been made to improve the basic properties of ferrites by substituting or adding various ions with different valence states depending on the applications of interest. Generally, the substitution of paramagnetic or diamagnetic ions in pure ferrites results in the modification of their structural, mechanical, electrical and magnetic properties [9,10]. Previous work showed that high initial magnetic permeability can be achieved only in samples with large grain size and residual porosity located at grain boundaries. And grain growth kinetics; however, depend strongly on the impurity content [11].

A minor additive in a host material can greatly change the nature and concentration of defects, which can affect the kinetics of grain growth, grain boundary motion, pore mobility and pore removal [12]. The presence of liquid phase during sintering facilitates the rearrangement due to the capillary

* Corresponding author at: School of Materials and Metallurgy, Northeastern University, 117, Box 110004 Shenyang, China. Tel.: +86 24 83686462; fax: +86 24 83682912.
E-mail address: djzneu@yahoo.cn (J. Du).

0272-8842/$36.00.
doi:10.1016/j.ceramint.2011.08.061

forces between particles. In order to apply liquid phase successfully during sintering of nickel ferrite ($NiFe_2O_4$) and optimize micro-structural evolution, the amount of liquid phase in samples during sintering must be carefully controlled [13,14]. V_2O_5 has a low melting point of 670 °C and liquid phase on the grain boundaries can promote sintering. Therefore it was the aim of this work to study the influence of V_2O_5 dopant on the microstructure, promoting sintering mechanism and magnetic properties of $NiFe_2O_4$ ferrite ceramics.

2. Experimental procedure

2.1. Synthesis

Samples of $NiFe_2O_4$ composite ceramics were made from a mixture of NiO and Fe_2O_3. The molar ratio of NiO to Fe_2O_3 was 1.87:1 in the mixture. In order to analyze the effects of V_2O_5 addition, samples with different amounts of this additive (i.e., $x = 0.5$, 1.0, 2.0, 2.5 wt%, respectively), were also prepared. Ceramic bodies were fabricated from high purity reagents [Fe_2O_3: 99.3% (Xincheng, China), NiO: 99.98% (Guoyao, China), V_2O_5: 97.5% (Guoyao, China)]. Raw materials (NiO power and Fe_2O_3 power) were ground in distilled water via a ball-milling using polypropylene jars with yttria-stabilized zirconia balls for 24 h. The mixture was dried at 120 °C for 12 h. Then the mixture was ground with 4 vol% polyvinyl alcohol (PVA) binder and pressed at 160 MPa into blocks (70 mm × 15 mm × 8 mm) using a stainless steel die. The blocks were calcined at 1000 °C in air for 6 h to produce the $NiFe_2O_4$ spinel matrix material. The calcined matrix products were crushed and ball-milled with different amounts of V_2O_5, a ball-milled process lasted for another 24 h with distilled water as dispersant, then the mixture was dried thoroughly. Adding 4 vol% PVA binders, the dried mixture was fabricated into 70 mm × 15 mm × 8 mm blocks by cold pressing at a pressure of 200 Mpa.

2.2. Sintering experiment

Sintering studies for the green blocks were performed in air in a vertical dilatometer (SETSYS18 EV-24, France). The dilatometer allowed continuous monitoring of axial shrinkage. During the sintering experiment, all samples were heated at a constant rate (say, 5 K/min) to a desired temperature and then furnace-cooled down to ambient temperature.

2.3. Characterization

Fracture surface for sintered samples was characterized using scanning electron microscope (SEM) (SSX-550, Japan). And the crystalline phases were identified by a D/max 2RB X-ray diffractometer (Japan) with Cu Kα radiation, pip voltage 40 kV and current 100 mA.

Measurements of various magnetic properties like saturation magnetization and coercivity were carried out in a vibrating sample magnetometer (VSM, Lakeshore 7400) at room temperature. And all samples for tests were cut into a shape (2 mm × 2.5 mm × 3 mm).

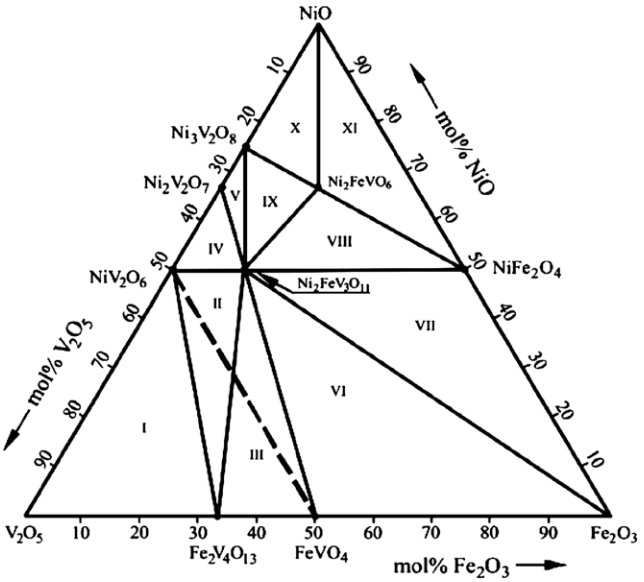

Fig. 1. Ternary phase diagram of NiO–V_2O_5–Fe_2O_3.

3. Results and discussion

3.1. Phase identification and microstructure

The ternary phase diagram of NiO–V_2O_5–Fe_2O_3 system [15] is shown in Fig. 1. All the compositions after reaction locate in XI region. Fig. 1 indicates that the phase composition located in XI region is Ni_2FeVO_6–NiO–$NiFe_2O_4$.

In order to further identify the phase transformation in sintered samples, X-ray diffraction patterns (XRD) of the synthesized ceramic powder with various amounts of V_2O_5 was also examined, the results are shown in Fig. 2. Three sets of different XRD patterns corresponding to $NiFe_2O_4$, NiO and Ni_2FeVO_6 phase can be indexed. And analysis of the different pattern of all samples confirmed the formation of spinel structure.

The SEM photographs for sintered ceramic samples doped with different amounts of V_2O_5 are shown in Fig. 3. It can be seen that the average grain size and/or the microstructure of

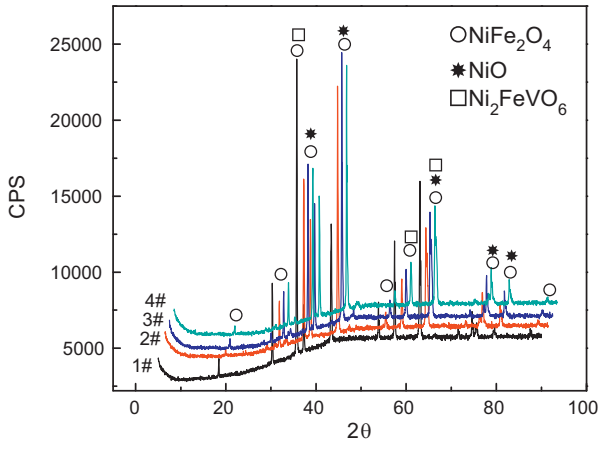

Fig. 2. XRD patterns of sintered ceramic samples with x wt% V_2O_5 (the value of x for 1#–4# samples is 0, 0.5, 1.0, 2.5 wt% respectively).

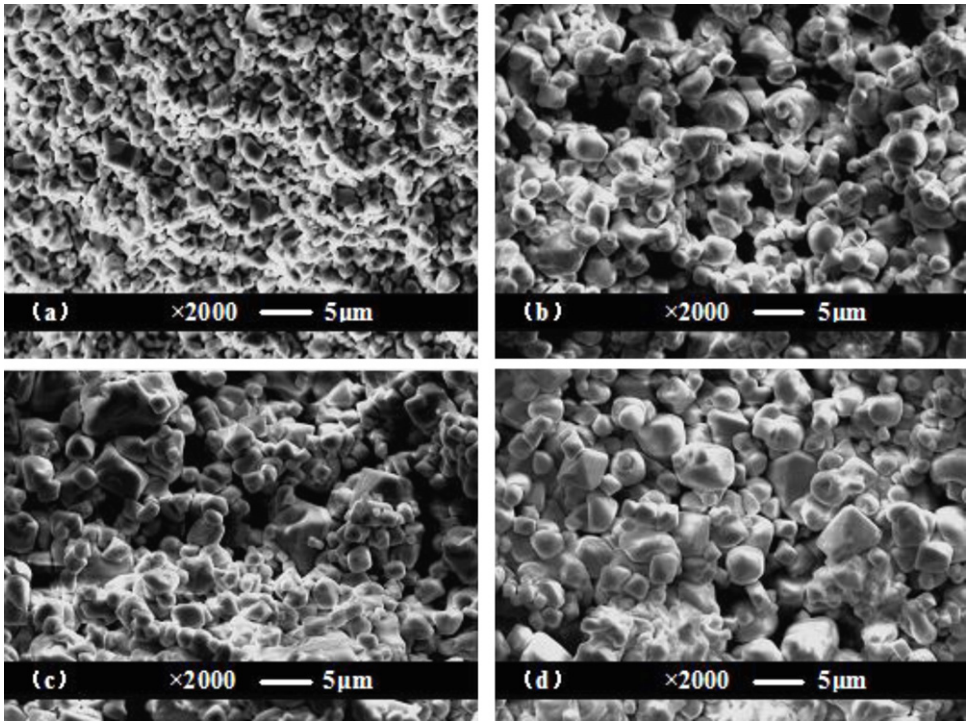

Fig. 3. Photomicrographs of sintered samples (1200 °C, 6 h) for samples 1#, 2#, 3#, 4#.

$NiFe_2O_4$ composite ceramics strongly depends on the amount of V_2O_5 in samples during sintering process. The un-doped $NiFe_2O_4$ ceramic is very porous (only 90.87% R.D.), the grain size (Fig. 3a) is uniform, being around 1–2 μm. However, 0.5 wt% V_2O_5 doping increases the crystallite size (Fig. 3b). The grain size is about 2–4 μm, and relative density (R.D.) reaches ~92.51%. Further more, the grain size is non-uniform. When the V_2O_5 content is up to 1.0 wt%, apparent sintering trajectories can be detected, as shown in Fig. 3c. The grain size is similar to that of 0.5 wt% V_2O_5 doped ceramic samples, and the relative density exhibits a slightly increase up to 92.85%.

When 2.5 wt% V_2O_5 was introduced into the matrix, the grain size accretes obviously. The relative density can reach 94.3% and grain size is also non-uniform, being almost 3–5 μm. It indicates that a small amount of V_2O_5 doping increase the densification of $NiFe_2O_4$ ceramic matrix, and promotes the grain growth.

3.2. Analysis of non-isothermal sintering behavior

A constant heating rate, i.e., 5 K/min was used to study the non-isothermal sintering behavior of NiO–V_2O_5–Fe_2O_3 system here. The linear shrinkage ($\Delta L/L_0$) of un-doped and V_2O_5-doped ceramic samples sintered at a constant heating rate of 5 K/min is shown in Fig. 4. The addition of V_2O_5 shifts the onset of sintering towards lower temperatures from ~990 °C for un-doped samples to ~660 °C for 2.5 wt% V_2O_5-doped samples. It can also be seen from Fig. 4 that the introduction of V_2O_5 is beneficial to enhancement of linear shrinkage from 10.84% to 16.08% with a doping range from 0 wt% to 2.5 wt%.

Fig. 5 shows the linear shrinkage rate ($d(\Delta L/L_0)/dt$) as a function of temperature for different V_2O_5 contents. It is observed that there is an obvious decrease in the temperature of maximum shrinkage rate (T_{max}) with an increase in V_2O_5 content. For example, the temperature of maximum shrinkage rate decreases from 1207 °C for un-doped samples to 1148 °C for 2.5 wt% V_2O_5-doped samples. The difference in the values of T_{max} for both samples is near to 60 °C. These results suggest that MnO_2 doping can reduce the sintering temperature dramatically.

In addition, sintering mechanism and apparent activation energy are also studied. According to the suggestion by Woolfrey et al. [16], three different heating rates, i.e., 5, 10 and 20 K/min, were adopted to determine sintering mechanism and calculate apparent activation energy, Q. In Ref. [17], the method to determine sintering mechanism was given in forms of Equations 1–6 in Model 1. Sintering mechanism is

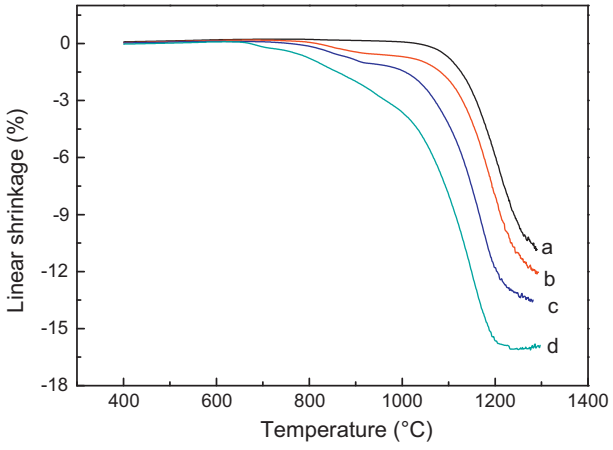

Fig. 4. Linear shrinkage versus sintering temperature for (a) un-doped samples, (b) 0.5, (c) 1.0 and (d) 2.5 wt% V_2O_5-doped ceramic samples sintered at a heating rate of 5 K/min.

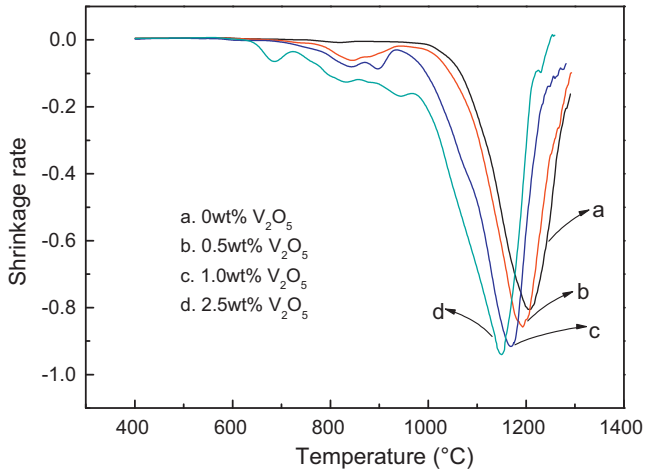

Fig. 5. Shrinkage rate against sintering temperature for (a) un-doped sample, (b) 0.5, (c) 1.0 and (d) 2.5 wt%. V_2O_5-doped ceramic samples sintered at a heating rate of 5 K/min.

characterized by values of power *m*. The activation energy, *Q*, and exponent, *m* of $NiFe_2O_4$ ceramics with different amounts of V_2O_5 obtained are listed in Table 1.

According to definition of different sintering mechanisms by Bannister [18] cited in Ref. [17], it can be assumed that the early-stage synthesis process of $NiFe_2O_4$ should be mainly controlled by grain boundary diffusion. When V_2O_5 addition was introduced into the ceramic matrix, an obvious change in the power law m can be observed, as shown in Table 1. With increasing V_2O_5 up to 2.5 wt%, the value of the power law *m* is 1.05. It can be concluded that it should be volume-diffusion controlled sintering for samples with 2.5 wt% V_2O_5 addition. With 0.5 wt% and 1.0 wt% V_2O_5 addition, the power laws *m* are 1.47 and 1.30, respectively. The early-stage sintering processes for the two may be controlled by both grain boundary diffusion and volume-diffusion mechanisms. In addition, it is interesting to note that with an increase of V_2O_5 addition in the range from 0 wt% to 2.5 wt%, the apparent activation energy decreased from 813.919 kJ/mol to 298.806 kJ/mol. And according to Ref. [15], the formation of Ni_2FeVO_6 has a lower melting point of 670 °C. When the sintering temperature was up to 1200 °C, it changed into liquid phase to produce capillary force, which was beneficial to the rearrangements of particles. It acted as liquid-phase

Table 1
Power law *m*, and activation energy *Q* based on Equation 5, for the ceramic samples with different compositions.

Compositions	*m*	*Q* (KJ/mol)
Un-doped samples	2.06	813.919
0.5 wt% V_2O_5 doping	1.47	619.578
1.0 wt% V_2O_5 doping	1.30	431.361
2.5 wt% V_2O_5 doping	1.05	298.806

sintering aid to accelerate the densification of ceramic matrix. Simultaneously, the ionic radius of V^{5+} ions is 0.059 nm. It is smaller than those of Fe^{3+} and Ni^{2+} ions. So lattice distortion could be detected during synthesis process. It may promote the sintering for the ceramic matrix. The analysis above, suggests that the introduction of V_2O_5 could promote the sintering process.

3.3. Magnetic properties

Magnetization measurements for all the ceramic samples with different compositions were carried out at 300 K by a high field hysteresis loop technique [19]. All the tested samples were heated to 1200 °C with a heating rate of 10 K/min, were sintered in air for 6 h and then cooled down to ambient temperature. The curves of magnetization versus applied field for ceramic samples with different amounts of V_2O_5 (① 0 wt%; ② 0.5 wt%; ③ 1.0 wt%; ④ 2.5 wt%) are shown in Fig. 6. The value of coercivity Hc, saturation magnetization Ms and the remnant ratio $R = Mr/Ms$ for ceramic samples is listed in Table 2.

After introduction of V_2O_5 into the ceramic matrix, the saturation magnetization (Ms) decreases. It mainly caused by the generation of Ni_2FeVO_6, as shown in Fig. 2, which decreased the content of $NiFe_2O_4$. The remnant ratio Mr/Ms is a characteristic parameter of the material. High remnant ratio is an indication of the ease with which the direction of magnetization reorients to nearest easy axis magnetization direction after the magnetic field is removed. The lower value of remnant ratio is indication of isotropic nature of material. It is observed from Table 2 that the values of remnant ratio in the present case are in a range from 0.0724 to 0.203 and show increasing trend with V_2O_5 addition. It can be seen from Table 2

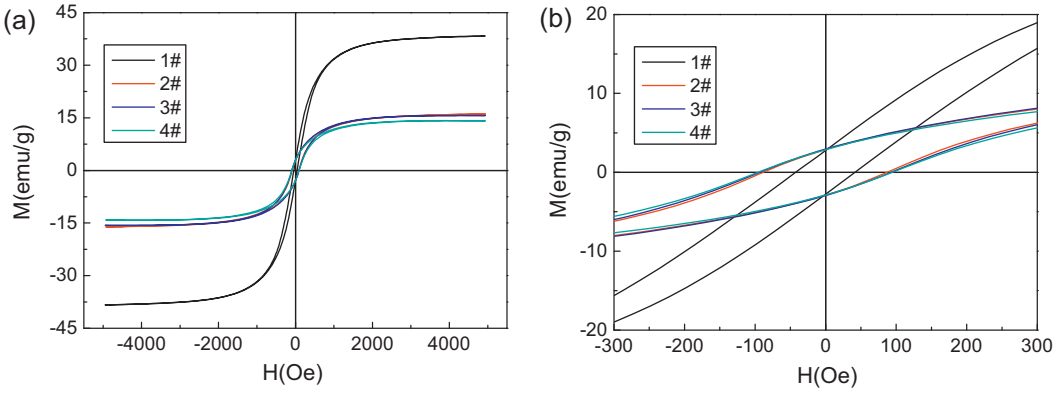

Fig. 6. Magnetic hysteresis loops for ceramic samples doped with various amounts of V_2O_5. (b) A part of magnetic hysteresis loops for (a).

Table 2
Magnetic data of V_2O_5-doped $NiFe_2O_4$ samples.

	1#	2#	3#	4#
Ms (emu/g)	38.337	16.099	15.671	14.190
Mr (emu/g)	2.777	2.882	2.943	2.879
Mr/Ms	0.0724	0.179	0.188	0.203
Hc (Oe)	32.346	51.384	52.284	56.811

that the coercivity (Hc) increases with raising V_2O_5 content from the whole aspect. The relationship between saturation magnetization and coercivity (Hc) was mentioned in Ref. [20], $Hc = 2K_1/\mu_0 Ms$. According to this relation Hc inversely proportional to Ms, it can be found this is consistent with our experimental results here. The value of coercivity (Hc) increases rapidly with V_2O_5 content. It may be attributed to the enhancement effect of V_2O_5 addition on crystallite sizes, which can be observed from Fig. 3. It can be seen from Table 2 that the values of coercivity for all composition are quite low ($Hc < 75$ Oe). This indicates that the studied samples retain soft ferrite nature with V_2O_5 addition.

4. Conclusions

Nickel ferrites doped with V_2O_5 have been synthesized through a two-step sintering process. X-ray diffraction of the prepared samples shows that $NiFe_2O_4$, NiO and Ni_2FeVO_6 phase are the main phases in sintered ceramic matrix. Introduction of V_2O_5 into the ceramic matrix is beneficial to promote sintering process. V_2O_5 can promote sintering process, the temperature for 2.5 wt% V_2O_5-doped samples to reach the maximum shrinkage rate is 59 °C lower than that of un-doped samples. With increasing V_2O_5 addition from 0 wt% to 2.5 wt%, the apparent activation energy decreased from 813.919 kJ/mol to 298.806 kJ/mol. The early-stage synthesis process of un-doped ceramic samples and 2.5 wt% V_2O_5-doped samples are mainly controlled by grain boundary diffusion and volume diffusion, respectively. The early-stage sintering processes for 0.5 wt% and 1.0 wt% V_2O_5-doped samples are controlled by both grain boundary diffusion and volume-diffusion mechanism. And the hysteresis loop study shows a decrease in the saturation magnetization (Ms) with increasing V_2O_5 content due to its enhancement effect on crystallite sizes. The residual magnetization ratio (Mr/Ms) and coercivities (Hc) increase in the range of V_2O_5 concentration from the whole aspect.

Acknowledgments

The authors gratefully acknowledge the financial support from the State Key Program of National Natural Science of China (Nos. 50834001, 50971038) and National High Technology Research and Development Program of China (863 Program) (No. 2009AA03Z502). The authors also thank for Professor Gaowu Qin, School of Materials and Metallurgy for utilizing the research facilities available in VSM.

References

[1] S.E. Shirsath, B.G. Toksha, K.M. Jadhav, Structural and magnetic properties of In^{3+} substituted $NiFe_2O_4$, J. Mater. Chem. Phys. 117 (2009) 163–168.
[2] A.C.F.M. Costa, V.J. Silva, D.R. Cornejo, M.R. Morelli, R.H.G.A. Kiminami, L. Gama, Magnetic and structural properties of $NiFe_2O_4$ ferrite nanopowder doped with Zn^{2+}, J. Magn. Magn. Mater. 320 (2008) e370.
[3] Y.M. Al Angari, Magnetic properties of La-substituted $NiFe_2O_4$ via egg-white precursor route, J. Magn. Magn. Mater. 323 (2011) 1835–1839.
[4] A. Goldman, Modern Ferrite Technology, Marcel Dekker Inc., New York, 1993.
[5] S.P. Ray, Inert anodes for Hall cells [A], in: R.T. Miller (Ed.), Light Metals 1986 [C], 28, TMS, Warrendale, PA, 1986, pp. 7–298.
[6] E. Olsen, J. Thonstad, Nickel ferrite as inert anodes in aluminium electrolysis (part I): material fabrication and preliminary testing, J. Appl. Electrochem. 29 (1999) 293–299.
[7] D.R. Sadoway, Inert anodes for the Hall Hároult cell: the ultimate materials challenge, JOM 53 (2001) 34–35.
[8] D.R. Patil, B.K. Chougule, Effect of copper substitution on electrical and magnetic properties of $NiFe_2O_4$ ferrite, Mater. Chem. Phys. 117 (2009) 35–40.
[9] O.M. Hemeda, M.Z. Said, M.M. Barakat, Spectral and transport phenomena in Ni ferrite-substituted Gd_2O_3, J. Magn. Magn. Mater. 224 (2001) 132–142.
[10] M.A. Gabal, Y.M. Al Angari, Effect of diamagnetic substitution on the structural, magnetic and electrical properties of $NiFe_2O_4$, Mater. Chem. Phys. 115 (2009) 578–584.
[11] M.F. Yan, D.W. Johnson, Shape dependence of the coarsening behavior of niobium carbide grains dispersed in a liquid iron matrix, J. Am. Ceram. Soc. 61 (1978) 342.
[12] D.W. Ready, Mass transport and sintering in impure ionic solids, J. Am. Ceram. Soc. 49 (1966) 366.
[13] M. Drofenik, A. Znidarsic, D. Markovec, Influence of the addition of Bi_2O_3 on the grain growth and magnetic permeability of MnZn ferrites, J. Am. Ceram. Soc. 81 (1998) 2841–2848.
[14] L. Richard, D. Sonia, G.J. Pierre, H.J. Marc, Influence of V_2O_5 on the magnetic properties of nickel–zinc–copper ferrites, J. Magn. Magn. Mater. 312 (2007) 328–330.
[15] M. Kurzawa, A.B. Tabero, Phase equilibria in the system NiO–V_2O_5–Fe_2O_3 in subsolidus area, J. Therm. Anal. Calorim. 77 (2004) 65–73.
[16] J.L. Woolfrey, M.J. Bannister, Nonisothermal techniques for studying initial-stage sintering, J. Am. Ceram. Soc. 55 (1972) 390–394.
[17] T.S. Zhang, P. Hing, H.T. Huang, Early-stage sintering mechanisms of Fe-doped CeO_2, J. Mater. Sci. 37 (2002) 997–1003.
[18] M.J. Bannister, Shape sensitivity of initial sintering equations, J. Am. Ceram. Soc. 51 (1968) 548–553.
[19] S.J. Santosh, E.S. Sagar, B.G. Toksha, S.J. Shukla, K.M. Jadhav, Effect of cation proportion on the structural and magnetic properties of Ni–Zn ferrites nano-size particles prepared by co-precipitation technique, Chin. J. Chem. Phys. 21 (2008) 381–386.
[20] J.M.D. Coey, Rare Earth Permanent Magnetism, John Wiley and Sons, New York, 1996.